Generating and Characterization Loft Surface by Type-2-Bishop Frame in Isotropic Space

Wageeda Mohamed Mahmoud[1], Mohamed Abdellatif Soliman[2], Samar Abdel Hafez Moukhtar[3]*

[1,3]*Department of Mathematics, Faculty of Science, Aswan University, Aswan, Egypt; E-mail: samarmoukhtar@sci.aswu.edu.eg*

[2]*Department of Mathematics, Faculty of Science, Assiut University, Assiut, Egypt*

Abstracts: This paper aims to design and generate a loft surface using three distinct curves (Hermitee cubic curve, straight line, and quadratic Bezier curve) and analyze its characteristics in isotropic space using type-2-Bishop. Moreover, the loft surface's 1st and 2nd - fundamental forms in the loft surface were investigated. In addition, their Gaussian, mean, and second Gaussian curvatures in I^3 were computed using the first and second type-2-Bishop curvatures. Furthermore, the required and adequate conditions for the surface with type 2-Bishop curvatures that are developable, minimal, and Weingarten surfaces (W-surface) were furnished. Besides, based on our results, two applications were provided to create and design a loft surface in biology: a double helix DNA surface and a cusp surface and all the above properties (*I, II, H, K,* K_{11}, developable, minimal, and W-surface) were studied.

Keywords: Loft Surface, Isotropic Space, Quadratic Bezier Curve, Hermite Cubic Curve, Double Helix DNA Surface, Cusp Surface.

1. INTRODUCTION

The loft is a planar drawing obtained through the development of SMCs that incorporates manufacturing and inspection features before being transferred to astrofoil sheets and released for production [1]. This type of surface patch has a curved shape [2].

A surface that provides a smooth transition between two or more disconnected surfaces or links two or more separate, intersecting surfaces is referred to as a general lofting surface.

Lofting surfaces are frequently instructed on edges, corners, and joints. A lofting surface's main feature is that it provides a smooth transition between the surfaces it links with some degree of continuity. The way the lofting surface meets the main surfaces is typically more significant than the precise geometry of the interior [3].

Shipbuilders were historically one of the preliminary to automate both processes to construct surface representations. Ships are large, and sail lofts above the dockyard's drying docking area are the only large and suitable dry location in a dockyard for stockpiling comprehensive ship design parts. Lofted surfaces describe those areas of a ship's surface that seem flat in one direction and curled in the opposite direction. Automobile and aircraft manufacturers began to focus on using computers to automate vehicle creation and design in the 1960s. Customarily, illustrators and developers would have to create designs of any portion of a car or airplane's surface in clay, which were then utilized to produce workers by creating seal molds. Using a computer to build a surface portion cooperatively became possible and then let the computer drive a cutting machine to fabricate the portion [3]. While a loft is a solid or surface characteristic with more than two drawing profiles, a loft (or blend) surface is created rather than a ruled surface [4].

In computer-aided design (CAD), curves, surfaces, and solids can be created and designed with CAD in two-dimensional (2D) space as well as three-dimensional (3D) space. CAD is widely used in the automobile, boat building, and aviation industries, as well as in architecture and building for industry (building information modeling), prosthetics, and many other fields. Digital content creation (DCC) is a concept that refers to the formation of digital

animation for given effects in films, advertisements, and technical manuals in CAD. Even perfume bottles and shampoo dispensers are now created utilizing methods that would have been unthinkable to engineers in the 1960s due to the pervasiveness and power of computers in modern society [5, 6]. Computer-aided geometric design, specifically, refers to creating geometric models for item shapes (CAGD) [7]. A computer-aided drug design approach was used to create new norepinephrine transporter inhibitors as potential antipsychotic agents. Ten hypothetical inhibitors were created using computer-aided design and demonstrated superior pharmacological properties as potential antipsychotic agents compared to an FDA-approved antipsychotic drug (atomoxetine) [8].

Since curvature can disappear at some points along a curve $\varpi(r)$, when $\varpi''(r) = 0$, the Frenet-Serret frame does not exist for every point along each curve. Different frames are required in this instance [9]. Consequently, in 1975, Bishop introduced the Bishop frame using parallel vector fields. It is characterized as the parallel or alternative frame of curves. The Bishop frame, further recognized as the frame that enables paralleled transportation, is another method for describing the well-defined, and even though $\varpi''(r) = 0$, the frame is starting to move [10, 11]. Korpinar et al. procured several categorizations of parallel curves in E^3 using the Bishop frame [12]. An updated Bishop frame was presented as a regular curve known as a "Type-2 Bishop Frame" [13].

If a surface $\omega = R(J, p)$ for a pair of (J, p) by the KGaussian curvature, H mean curvature, and K_{II} second Gaussian curvature of a surface fulfills the condition $R(J, p) = 0$, where R is the Jacobi function described by $R = Jp - pJ$, then the surface is said to be a (J, p)-Weingarten surface (W-surface) [14,15].

2. FUNDAMENTAL CONCEPTS

Metrics and movement isotropic geometry is the three-dimensional affine transformation of a six-parameter function obtained by [16, 17]

$$\bar{U} = r_1 + u\ \cos\varepsilon - E\ \sin\varepsilon,$$

$$\bar{E} = r_2 + u\ \sin\varepsilon + E\ \cos\varepsilon,$$

$$\bar{L} = b_1 + b_2 U + b_3 E + L.$$

where $r_1,\ r_2,\ b_1,\ b_2,\ b_3, and\ \varepsilon\ \in \mathbb{R}$. The isotropic metric is generated by

$$ds^2 = dU^2 + dL^2 \qquad [1].$$

Let $O\ =\ (O_1,\ O_2,\ O_3)$ and $\varsigma = (\varsigma_1, \varsigma_2, \varsigma_3)$ be vectors in I^3. $\langle O, \varsigma \rangle_j$ of O and ς is defined as

$$\langle O, \varsigma \rangle_j = \begin{cases} O_3\varsigma_3 & if\ O_j = \varsigma_j = 0, \\ O_1\varsigma_1 + O_2\varsigma_2 & if\ otherwise. \end{cases} \qquad (2)$$

According to [18], the unit vector in isotropic space I^3 is given by $\mho = (0,0,1)$.

Along the unit speed curve ϖ, the Serret frame and type-2-Bishop frame are represented to $\{\mu,\ \Upsilon,\ S\}$ and $\{X,\ A,\ S\}$, respectively.

Frenet–Serret frame fulfills these equations:

$$\begin{cases} \dfrac{d\mu}{dt} = \kappa(t)\,\Upsilon(t), \\ \dfrac{d\Upsilon}{dt} = -\kappa(t)\,\mu(t)\ +\ \tau\,S(t), \\ \dfrac{dS}{dt} = -\tau\,\Upsilon(t). \end{cases} \qquad (3)$$

where κ and τ are the curvature and torsion of ϖ and

$$\mathrm{H}(\mu,\ \mu) = 1,\ \ H(\Upsilon,\ \Upsilon) = 1,\ \ \ H(\mathrm{S},\ \mathrm{S}) = 1,$$

$$\mathrm{H}(\mu,\ \Upsilon) = H(\Upsilon,\ \mathrm{S}) = H(\mu,\ \mathrm{S}) = 0.$$

The type 2-Bishop frame formula is described as

$$\begin{cases} X'(r) &= -\kappa_1(r)\ \mathrm{S}(r)\ , \\ A'(r) &= -\kappa_2(r)\ \mathrm{S}(r), \\ \mathrm{S}'(r) &= \kappa_1(r)\ X(r)\ + \kappa_2(r)\ A(r). \end{cases} \qquad (4)$$

where

$$\mathrm{G}(X,\ X) = 1,\ \ G(\mathrm{A},\ \mathrm{A}) = 1,\ \ \ G(\mathrm{S},\ \mathrm{S}) = 1,$$

$$\mathrm{G}(X,\ \mathrm{A}) = \mathrm{G}(\mathrm{A},\ \mathrm{S}) = \mathrm{G}(\mathrm{X},\ \mathrm{S}) = 0$$

Here the Bishop curvatures are defined by [9, 19]

$$\kappa_1(r) = \kappa(r)\ \cos\varepsilon\,(r), \qquad and\ \ \kappa_2(r) = \kappa(r)\ \sin\varepsilon\,(r).$$

where

$$\varepsilon = \tan^{-1}\left(\frac{\kappa_2(r)}{\kappa_1(r)}\right), \qquad \tau = \varepsilon', \qquad and\ \ \kappa(t) = \sqrt{\kappa_1^2(r) + \kappa_2^2(r)},$$

This formula describes the relationship and distinguishes among both Frenet and type-2-Bishop frames [11, 20]:

$$\begin{pmatrix} \mu(r) \\ \Upsilon(r) \\ S(r) \end{pmatrix} = \begin{pmatrix} sin\,\varepsilon\,(r) & -cos\,\varepsilon\,(r) & 0 \\ cos\,\varepsilon\,(r) & sin\,\varepsilon\,(r) & 0 \\ 0 & 0 & 1 \end{pmatrix} \begin{pmatrix} X(r) \\ A(r) \\ S(r) \end{pmatrix}$$

We defined a surface $\aleph$ in I^3 by

$$\sigma(y,w) = \big(\sigma_1(y,w),\ \ \sigma_2(y,w),\ \ \sigma_3(y,w)\big), \qquad (5)$$

For a surface $\sigma(y,w)$, the first fundamental form is determined concerning the induced metric as [11]

$$\mathrm{I} = \eth_{11}\ dy^2 + \eth_{12}\ dy\ dw + \eth_{22}\ dw^2,$$

where

$$\eth_{11} = \langle \sigma_y,\ \ \sigma_y \rangle, \qquad \eth_{12} = \langle \sigma_y,\ \ \sigma_w \rangle, \qquad \eth_{22} = \langle \sigma_w,\ \ \sigma_w \rangle \qquad (6).$$

The II is described for the normal vector field $\mho$ of a completely isotropic surface by [11]:

$$II = h_{11}\ dy^2 + h_{12}\ dy\ dw + h_{22}\ dw^2,$$

where

$$h_{11} = \langle \sigma_{yy}, \mho \rangle,\ \ h_{12} = \langle \sigma_{yw}, \mho \rangle,\ \ h_{22} = \langle \sigma_{ww}, \mho \rangle \qquad (7).$$

The definitions of an isotropic Gaussian curvature K, the isotropic mean curvature H, and the isotropic second Gaussian curvature K_{11} [11] are:

$$K(y,w) = \kappa_1\kappa_2 = \frac{h_{11}h_{22} - h_{12}^2}{\eth_{11}\eth_{22} - \eth_{12}^2}, \quad (8)$$

$$H(y,w) = \frac{1}{2}(\kappa_1 + \kappa_2) = \frac{\eth_{11}h_{22} - 2\eth_{12}h_{12} + \eth_{22}h_{11}}{2(\eth_{11}\eth_{22} - \eth_{12}^2)}, \quad (9)$$

$$K_{11}(y,w) = \frac{1}{(h_{11}h_{22} - h_{12}^2)^2}\left\{\begin{vmatrix} -\frac{1}{2}h_{11ww} + h_{12yw} - \frac{1}{2}h_{22yy} & \frac{1}{2}h_{11y} & h_{12y} - \frac{1}{2}h_{11w} \\ h_{12w} - \frac{1}{2}h_{22y} & h_{11} & h_{12} \\ \frac{1}{2}h_{22w} & h_{12} & h_{22} \end{vmatrix} - \begin{vmatrix} 0 & \frac{1}{2}h_{22y} & \frac{1}{2}h_{22w} \\ \frac{1}{2}h_{22y} & h_{11} & h_{12} \\ \frac{1}{2}h_{22w} & h_{12} & h_{22} \end{vmatrix}\right\}. \quad (10)$$

In section 3, we studied how to generate the loft surface.

3. LOFT OR (BLEND) SURFACE IN I^3

As illustrated in Figure (1), the A loft surface could be decided to make by three curves $\varphi(y)$, $\mathcal{M}(y)$, and $\mathbb{Q}(y)$, as in the w position, on three different concurrent drawing planes [4].

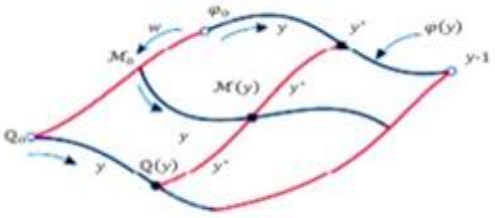

Figure1: Quadratic surfaces lofted in the w direction by $\varphi(y)$, $\mathcal{M}(y)$, and $\mathbb{Q}(y)$ [4].

Unless assuming that the curve $\mathcal{M}(y)$ is at w =1/2 of such loft surface, any curve anywhere along the w path produced by a fixed y value at the three separate curves [4].

In this work, we discussed the loft surface designed by three curves. For all y, w the values in $(0,1)$; so, the parametric equation of the loft surface is as follows:

$$\sigma(y,w) = [w^2 \quad w \quad 1]\begin{bmatrix} 2 & -4 & 2 \\ -3 & 4 & 1 \\ 1 & 0 & 0 \end{bmatrix}\begin{bmatrix} \varphi(y) \\ \mathcal{M}(y) \\ \mathbb{Q}(y) \end{bmatrix}, \quad (y,\ w) \in [0,1] \times [0,1] \quad (11)$$

In addition, we discussed constructing the three curves to get to the final surface equation.

We selected Hermite's cubic curve $\varphi(y)$, the first curve in the loft surface. A cubic curve is described by its start and end points and the tangent vectors at those points. This is recognized as the geometric format curve [4].

The formula of the Hermite cubic curve is given by:

$$\varphi(y) = [y^3 \quad y^2 \quad y \quad 1]\begin{bmatrix} 2 & -2 & 1 & 1 \\ -3 & 3 & -2 & 0 \\ 0 & 0 & 1 & 0 \\ 1 & 0 & 0 & 0 \end{bmatrix}\begin{bmatrix} \varphi_0(y) \\ \varphi_1(y) \\ \varphi_{0,y}(y) \\ \varphi_{1,y}(y) \end{bmatrix}, \quad (12)$$

Choosing the points and the vectors are defined by:

$$\varphi_0(y) = (1,\ 0,\ 0), \qquad \varphi_1(y) = (0,\ 0,\ 0),$$
$$\varphi_{0,y}(y) = (0,-1,0), \quad \varphi_{1,y}(y) = (2,-2,\ 0). \quad (13)$$

By Eq. (12), we constituted the Hermite cubic curve by the following equation:

$$\varphi(y) = (1 - y^2,\ -y,\ 0) \quad (14)$$

We chose the second curve $\mathcal{M}(y)$ as a straight line in the loft surface (4). The following equation was utilized to choose the two points $\mathcal{M}_0(y) = (-1, 0, \frac{1}{2})$ and $\mathcal{M}_1(y) = (0, -\frac{1}{4}, 1)$ to establish a straight line as:

$$\mathcal{M}(y) = (1-y)\,\mathcal{M}_0(y) + y\,\mathcal{M}_1(y) = \left(-1,\ -\frac{1}{4}\,y,\ -1+\frac{1}{2}\,y\right) \quad (15)$$

The quadratic Bezier curve is the third curve on the surface. Pierre Bezier devised one such curve in the 1970s, which has since been one of the most widely used curves in geometric modeling [4].

A quadratic Bezier curve is described as follows:

$$\mathbb{Q}(y) = \sum_{j=0}^{n} \mathbb{Q}_j\, \mathcal{B}_{j,m}(y), \quad y \in [0,1] \quad (16)$$

for which y_j is the i[th] control point, m is the curve's polynomial order, and $\mathcal{B}_{j,m}$ is the corresponding Bernstein polynomial described as:

$$\mathcal{B}_{j,m}(y) = L(m,j)y^j(1-y)^{m-j}, \quad y \in [0,1] \quad (17)$$

$L(m,j)$ is the binomial coefficient defined as:

$$L(m,j) = \frac{m!}{j!\,(m-j)!}$$

At $m = 3$, the curve is characterized by four control points for a quadratic Bezier curve. The basic functions of a quadratic curve can be inferred from Eq. (16) as follows:

$$\mathcal{B}_{0,3}(y) = (1-y)^3,$$

$$\mathcal{B}_{1,3}(y) = 3\,y^3\,(1-y)^2,$$

$$\mathcal{B}_{2,3}(y) = 3\,y^2\,(1-y),$$

$$\mathcal{B}_{3,3}(y) = y^3.$$

As illustrated in Eq. (17), a quadratic Bezier curve can be expressed as:

$$\mathbb{Q}(y) = \sum_{j=0}^{3} \mathbb{Q}_j\,\mathcal{B}_{j,3}\,(y) = \mathbb{Q}_0\,\mathcal{B}_{0,3}(y) + \mathbb{Q}_1\,\mathcal{B}_{1,3}(y) + \mathbb{Q}_2\,\mathcal{B}_{2,3}(y) + \mathbb{Q}_3\,\mathcal{B}_{3,3}(y)$$
$$= (1-y)^3 + 3\,y^3\,(1-y)^2 + 3\,y^2\,(1-y) + y^3\,, \qquad y \in [0,1] \qquad (18)$$

It should be mentioned that Eq. (18) can also be authored by the Bezier curve in matrix form as:

$$\mathbb{Q}(y) = \begin{bmatrix} y^3 & y^2 & y & 1 \end{bmatrix} \begin{bmatrix} -1 & 3 & -3 & 1 \\ 3 & -6 & 3 & 0 \\ -3 & 3 & 0 & 0 \\ 1 & 0 & 0 & 0 \end{bmatrix} \begin{bmatrix} \mathbb{Q}_0(y) \\ \mathbb{Q}_1(y) \\ \mathbb{Q}_2(y) \\ \mathbb{Q}_3(y) \end{bmatrix}, \qquad (19)$$

By choosing the points

$$\mathbb{Q}_0(y) = (1,\ 0,\ -1), \qquad \mathbb{Q}_1(y) = \left(1,\ 0,\ -\frac{2}{3}\right),$$
$$\mathbb{Q}_2(y) = \left(1,\ 0,\ -\frac{1}{3}\right), \quad \mathbb{Q}_3(y) = (-2,\ 0,\ 0) \qquad (20)$$

From Eq. (20), we substituted in Eq. (19) to get the equation of the Bezier curve

$$\mathbb{Q}(y) = (1 + y^2,\ 0,\ -1 + y) \qquad (21)$$

From Eqs. $(14), (15)$ and (21), we concluded the loft surface as defined by Eq. (11) as:

$$\sigma(y,w) = \left(-1 + 2\,y^2 w - y^2\ ,\ -w - y + w^2 y\ ,\ 2\,w^2 - 2\ y\,w\right) \qquad (22)$$

The properties of the loft surface are investigated in the following section.

4. THE PROPERTIES OF LOFT SURFACE IN I^3

In the present section, the loft surface obtained by the vectors $X(s),\ A(s),\ \text{and}\ O(s)$ within the type-2-Bishop frame is presented as:

$$\sigma(y,w) = \left(-1 + 2\,y^2 w - y^2\right) X(s) + \left(-w - y + w^2 y\right) A(s) + \left(2\,w^2 - 2\ y\,w\right) O(s) \qquad (23)$$

The figure of the loft surface is shown in Figure 2.

Figure 2: The Loft Surface

To calculate the first fundamental form of $\aleph$, we have to find the first derivative of the surface by the following:

$$\sigma_y(y,w) = \Big(2y(-1+2w) + w(-3+y+2w)\,\kappa_1(y),\ -1+w^2+w(-3+y+2w)\,\kappa_2(y),\\ w + \big(1+y^2(1-2w)\big)\kappa_1(y) + (y+w-yw^2)\,\kappa_2(y)\Big), \quad (24)$$

$$\sigma_w(y,w) = (2y^2,\ -1+2y\,w,\ -3+y+4w). \quad (25)$$

From Eqs. (6), (23), (24), and (25), we got the coefficients of the I from:

$$\wp_{11} = \big(2y(-1+2w) + w(-3+y+2w)\,\kappa_1(y)\big)^2 + \big(-1+y\,w\,\kappa_2(y)\big)^2,$$

$$\wp_{12} = -2y(y-w)\big(y(2-4w) + w^2 + y\,w\,\kappa_1(s)\big), \quad \wp_{22} = 4y^2(y-w)^2.$$

To find the II form of $\aleph$, we must find the second derivative of the surface by the following formula:

$$\sigma_{yy}(y,w) = \Big(-2+4w+\kappa_1(y)\ \big(2w + \big(1+y^2(1-2w)\big)\kappa_1(y) + (y+w-y\,w^2)\kappa_2(y)\big)\\ + w(-3+y+2w)\kappa_1{}'(y),\ \big(2w + (1+y^2-2y^2w)\kappa_1(y)\big)\kappa_2(y)\\ + (y+w-yw^2)\kappa_2(y)^2 + w(-3+y+2w)\kappa_2{}'(y),\ 4y(1-2w)\kappa_1(y) - w(-3+y\\ + 2w)\kappa_1(y)^2 - 2(-1+w^2)\kappa_2(y) - w(-3+y+2w)\kappa_2(y)^2 + (1+y^2-2y^2w)\kappa_1{}'(y)\\ + (y+w-yw^2)\kappa_2{}'(y)\Big) \quad (27)$$

$$\sigma_{ww}(y,w) = (0,\ 2y,\ 0) \quad (28)$$

$$\sigma_{yw}(y,w) = \Big(4y + (-3+y+4w)\kappa_1(y),\ 2w + (-3+y+4w)\kappa_2(y),\ 1+\kappa_2(y)\\ - 2y\big(y\kappa_1(y) + w\kappa_2(y)\big)\Big) \quad (29)$$

From Eqs. (7), (27), (28), and (29), we obtained the second fundamental coefficients from:

$$h_{11} = 4y(1-2w)\,\kappa_1(y) - w(-3+y+2w)\kappa_1(y)^2 - 2(-1+w^2)\kappa_2(y) - w(-3+y+2w)\kappa_2(y)^2\\ + (1+y^2-2y^2w)\,\kappa_1{}'(y) + (y+w-y\,w^2)\kappa_2{}'(y), \quad (30)$$

$$h_{12} = 1 + \kappa_2(y) - 2y\left(y\,\kappa_1(y) + w\,\kappa_2(y)\right), \qquad h_{22} = 0. \tag{31}$$

From Eqs. (8), (9), and equations of fundamental forms, we concluded the Gaussian curvature and mean curvature as:

$$K(y,w) = \frac{-\left(1 + \kappa_2(y) - 2y\left(y\,\kappa_1(y) + w\,\kappa_2(y)\right)\right)^2}{\left(-2y\left(1 + y - 2w + y\,w(-2+3w)\right) + w(-3+y+2w)\left((1-2y\,w)\kappa_1(y) + 2y^2\kappa_2(y)\right)\right)}, \tag{32}$$

$$H(y,w) = \frac{1}{\left(-2y\left(1 + y - 2w + y\,w\,(-2+3w)\right) + w\,(-3+y+2w)\left((1-2y\,w)\,\kappa_1(y) + 2y^2\kappa_2(y)\right)\right)}$$

$$\left(\left(-2\left(1 + \kappa_2(y) - 2y\left(y\,\kappa_1(y) + w\,\kappa_2(y)\right)\right)\left(2y^2\left(2y\,(-1+2w) + w\,(-3+y+2w)\kappa_1(y)\right)\right.\right.$$
$$+ (-1+2y\,w)\left(-1 + w^2 + w(-3+y+2w)\kappa_2(y)\right)\Big)$$
$$+ (4y^4 + (1-2y\,w)^2)\left(4y(1-2w)\kappa_1(y) - w(-3+y+2w)\kappa_1(y)^2\right.$$
$$- 2(-1+w^2)\,\kappa_2(y) - w(-3+y+2w)\kappa_2(y)^2 + (1+y^2-2y^2w)\kappa_1{}'(y)$$
$$\left.\left.+ (y + w - y\,w^2)\,\kappa_2{}'(y)\right)\right)\right) \tag{33}$$

$$K_{11}\,(y,w) = \frac{1}{(-1+2y^2\kappa_1(y) + (-1+2y\,w)\,\kappa_2(y))^3}\Big(-4y^2\kappa_1(y)^3 + \kappa_1(y)^2\left(2 + (-2+y)(-1+y)\,\kappa_2(y)\right)$$
$$+ \kappa_2(y)\left(\kappa_2(y)\left(2 + 4y\,w + (-2+y)(-1+y)\,\kappa_2(y)\right) + 2y^3\,\kappa_1{}'(y)\right)$$
$$+ y\left(-1 + (-2+4y\,w)\,\kappa_2(y)\right)\kappa_2{}'(y)$$
$$+ 2y^2\kappa_1(y)\left(-2\left(-2 + k_2(y)\right)\kappa_2(y) + y\,\kappa_2{}'(y)\right)\Big), \tag{34}$$

In Figures 3 and 4, we demonstrated the effect of both Gaussian and mean curvatures on ℵ.

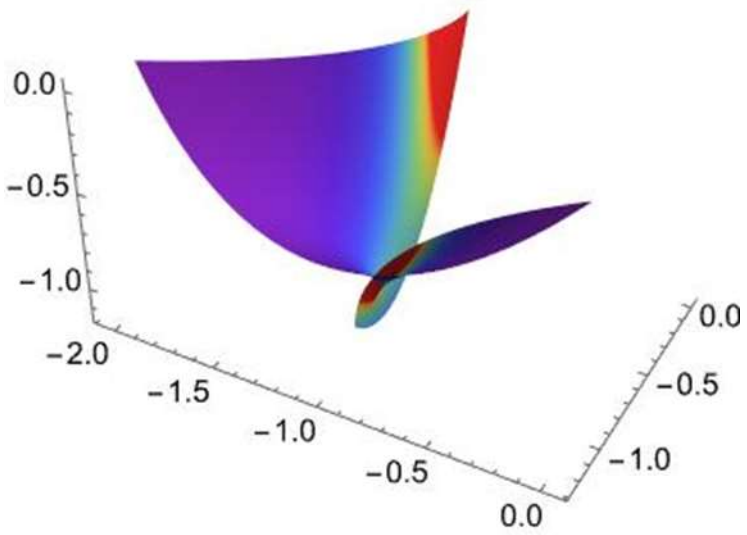

Figure 3: The Gaussian curvature is not defined at zero in a large percent and decrease from range between -2 and - 8 with a gradation of colors between yellow to dark magenta.

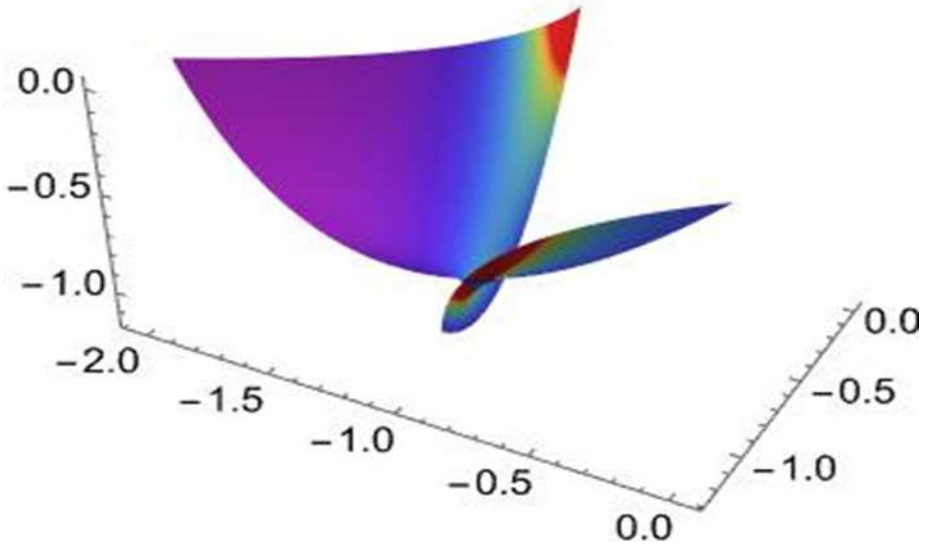

Figure 4: The mean curvature is not defined at zero and decreases between -2 and -8 with a gradation of colors between yellow to dark magenta.

The results of this paper are discussed in the next section.

5. RESULTS

We will discuss the following theorems:

Theorem (1): Let $\sigma = \sigma(y, w)$ be the loft surface in I^3 is a minimal under the following condition holds,

$$\kappa_2(y) = \frac{2y^2\kappa_1(y) - 1}{2y}$$

Proof: Let ϖ be a curve on the surface $\sigma(y,w)$. From Eq. (33), we satisfy $H(y,w) = 0$ by the loft surface. We get that:

$$\begin{aligned}\Big(\Big(-2\big(1+\kappa_2(y) - 2y\big(y\,\kappa_1(y) + w\,\kappa_2(y)\big)\big)\Big(2y^2\big(2y\,(-1+2w) + w\,(-3+y+2w)\kappa_1(y)\big)\\ + (-1+2y\,w)\big(-1+w^2+w(-3+y+2w)\kappa_2(y)\big)\Big)\\ + (4y^4 + (1-2y\,w)^2)\big(4y(1-2w)\kappa_1(y) - w(-3+y+2w)\kappa_1(y)^2\\ - 2(-1+w^2)\,\kappa_2(y) - w(-3+y+2w)\kappa_2(y)^2 + (1+y^2-2y^2w)\kappa_1{}'(y)\\ + (y+w-y\,w^2)\,\kappa_2{}'(y)\big)\Big)\Big) = 0 \qquad (35)\end{aligned}$$

By using the Mathematica program to solve (35), we have

$$\kappa_2(y) = \frac{2y^2\kappa_1(y) - 1}{2y}$$

that fulfill a minimal surface.

The following theorem (2) will be covered when the surface is developable.

Theorem (2): Let ϖ be a curve reference to type-2-Bishop frame in isotropic 3-space I^3. The isotropic loft surface $\sigma(y,w)$ is developable provided that the following condition is:

$$\kappa_2(y) = \frac{1-2y^2\,\kappa_1(y)}{-1+2\,y\,w}.$$

Proof: The lofting surface satisfies $K(y,w) = 0$, requirements Eq. (9) reveals what we can infer:

$$0 = \frac{-\big(1+\kappa_2(y) - 2y\big(y\,\kappa_1(y) + w\,\kappa_2(y)\big)\big)^2}{\big(-2y\big(1+y-2w+yw(-2+3w)\big) + w(-3+y+2w)\big((1-2yw)\kappa_1(y) + 2y^2\kappa_2(y)\big)\big)},$$

Then we have

$$1+\kappa_2(y) - 2y\big(y\,\kappa_1(y) + w\,\kappa_2(y)\big) = 0 \Rightarrow \kappa_2(y) = \frac{1-2y^2\,\kappa_1(y)}{-1+2\,y\,w}$$

By this condition, the $\sigma(y,w)$ is a developable surface.

The Weingarten surface can be studied by theorem (3).

Theorem (3): The isotropic loft surface is the (K,H) Weingarten surface under the conditions $\kappa_2(y) = \frac{1-2y^2\,\kappa_1(y)}{-1+2\,y\,w}$.

Proof: Weingarten isotropic surface satisfies Jacobi equation, $K_w H_y - K_y H_w$. If we drive the Eqs. (32) and (33) by y and w, respectively, and apply the Jacobi, then we get the following condition

$$\kappa_2(y) = \frac{1 - 2y^2\,\kappa_1(y)}{-1 + 2\,y\,w} \qquad (36)$$

When the condition (36) is fulfilled in the third theorem, the loft surface will be called the (K, H) Weingarten surface.

We noticed from theorems (2) and (3) that the loft surface is a Weingarten developable surface under condition (36).

Theorem (4): Let ϖ be a loft surface in I^3 parametrized by (23) and having a non-degenerate second fundamental form is a (K_{11}, K) W-surface if $\kappa_1(s) = 0$ and $\kappa_2(y) = \frac{1}{-1+2y\,w}$.

Proof: Assume ϖ is an I^3 loft surface parametrized by a type-2-Bishop frame (24). Using Mathematica, we calculated $(K_{11})_y$, $(K_{11})_w$, K_y, and K_w.

The lofting surface in I^3 satisfying the Jacobi equation is considered:

$$\emptyset(K_{11}, K) = (K_{11})_y\,K_w - (K_{11})_w\,K_y = 0,$$

concerning the Gaussian and second Gaussian curvatures K and K_{11}, respectively.

Then, we get $\kappa_1(y) = 0$ and $\kappa_2(y) = \frac{1}{-1+2y\,w}$.

6. APPLICATIONS OF LOFT SURFACE

This section shows how to deduce two applications of the double helix and a cusp as a lofted surface.

6.1. Double Helix DNA Surface

The much more essential genomic framework in biology is deoxyribonucleic acid (DNA). Its double-helical structure has come to represent the remarkable advances achieved in molecular biology within the last century. Even though Watson and Crick's model-building study predicted the double-helix structure more than seven decades ago, little is known about DNA's detailed structure, dynamics, and energetics, despite its pivotal role in all living systems [21]. The three-dimensional structure of DNA was not obtained until 1981 from single-crystal diffraction [22]. James Watson and Francis Crick correctly identified the 3-dimensional double helix structure of DNA. Hydrogen bonds hold complementary bases together as a pair [23].

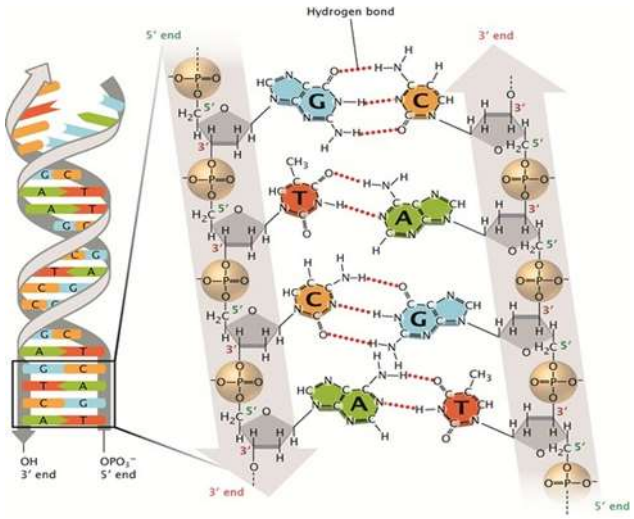

Figure 5: DNA's double-helical structure [23].

After all, furthermore, the two-dimensional parametric curve $(cos\ t, sin\ t)$ is a circle (one unit radius, centered on the origin). Consequently, the three-dimensional curve $(cos\ t, sin\ t, t)$ is a helix curving upward from the origin around the z-axis. The comparable curve $(cos(t+\pi), sin(t+\pi), t)$ is another helix, 180 degrees out of step with the first. These are the two boundary curves of a lofted surface, and all surfaces are created as a linear relationship between the two curves [3]. After that:

$$\begin{aligned} \boldsymbol{P}(y,w) = {} & (cos\ (y), \sin(y)\ , y)(1\ -\ w) + \ (cos(y+\pi), sin(y+\pi), y\ )w \\ & = \big((1\ -\ w)\cos(y) + w\ cos(y+\pi),\ \ (1\ -\ w)\sin(y) + w\ sin(y+\pi),\ \ y\big) \end{aligned} \qquad (37)$$

Here y can contain any value, and w can range from $0 \le w \le 1$. The surface resembles a twisted thread because of the double helix formed by the two curves [4].

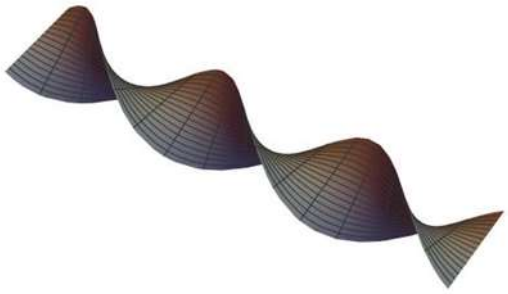

Figure 6: The double helix of a lofted surface.

We get some properties of a DNA lofted surface (first fundamental form, second fundamental form, mean curvature, Gaussian and second Gaussian curvatures, and Weingarten surface).

$$\wp_{11} = \big((-1+2w)\sin(y) + y\,\kappa_1(y)\big)^2 + \big(\cos(y) - 2w\ cos(y) + y\,\kappa_2(y)\big)^2,$$

$$\wp_{12} = -2y\ (\cos(y)\ \kappa_1(y) + \sin(y)\ \kappa_2(y)), \quad \wp_{22} = 4,$$

$$h_{11} = -y\left(\kappa_1^2(y) + \kappa_2^2(y)\right) + (-1+2w)\cos(y)\left(2\kappa_2(y) + \kappa_1'(y)\right) - (-1+2w)\sin(y)(2\,\kappa_1(y) - \kappa_2'(y)),$$

$$h_{12} = 2\left(\cos(y)\,\kappa_1(y) + \sin(y)\,\kappa_2(y)\right), \qquad h_{22} = 0,$$

$$H(y,w) = \frac{1}{(2(1-2w-y\sin(y)\,\kappa_1(y) + y\cos(y)\;\kappa_2(y))^2)}\left(y\cos(2y)\,\kappa_1^2(y) - y\cos(2y)\,\kappa_2^2(y) + 2\sin(y)\;\kappa_1(y)(1-2w+2y\cos(y)) + (-1+2w)\cos(y))(2\kappa_2(y) + \kappa_1'(y)\,\kappa_1'(y)) + (-1+2w)\sin(y)\,\kappa_2'(y)\right),$$

$$K(y,w) = -\frac{\left(\cos(y)\,\kappa_1(y) + \sin(y)\,\kappa_2(y)\right)^2}{\left(1-2w-y\sin(y)\;\kappa_1(y) + y\;\cos(y)\,\kappa_2(y)\right)^2}.$$

The DNA double helix surface is a (H, K) Weingarten surface under the condition:

$$\frac{\kappa_1(y)}{\kappa_2(y)} = -\tan y.$$

The Gaussian and mean curvatures of the DNA double helix surface are presented in Figures 7 and 8, respectively.

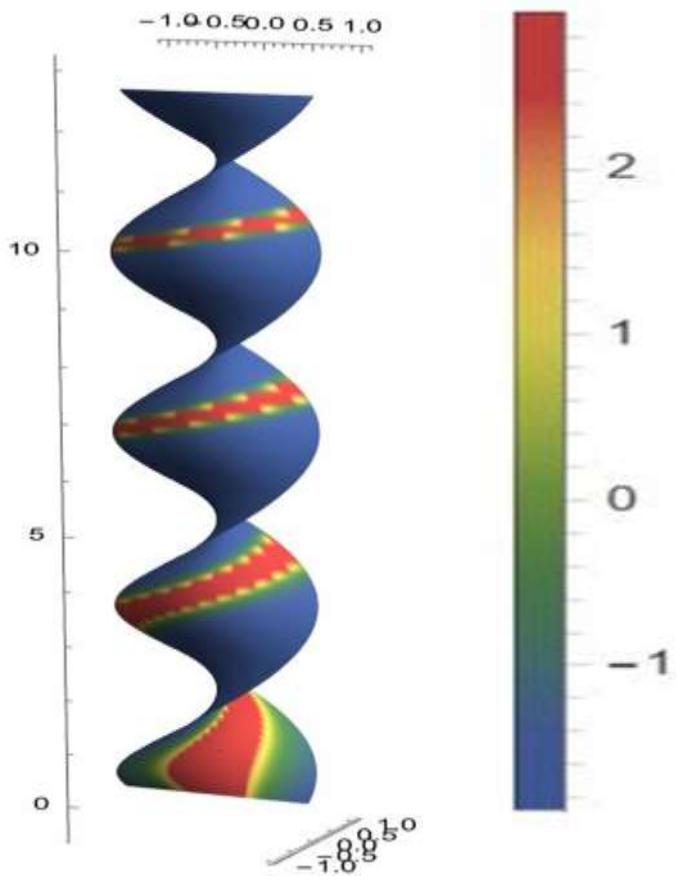

Figure 7: Gaussian DNA double helix curvature increases between orange and olive drab color, reaches a nihilistic zero, and decreases through dark green and midnight blue colors.

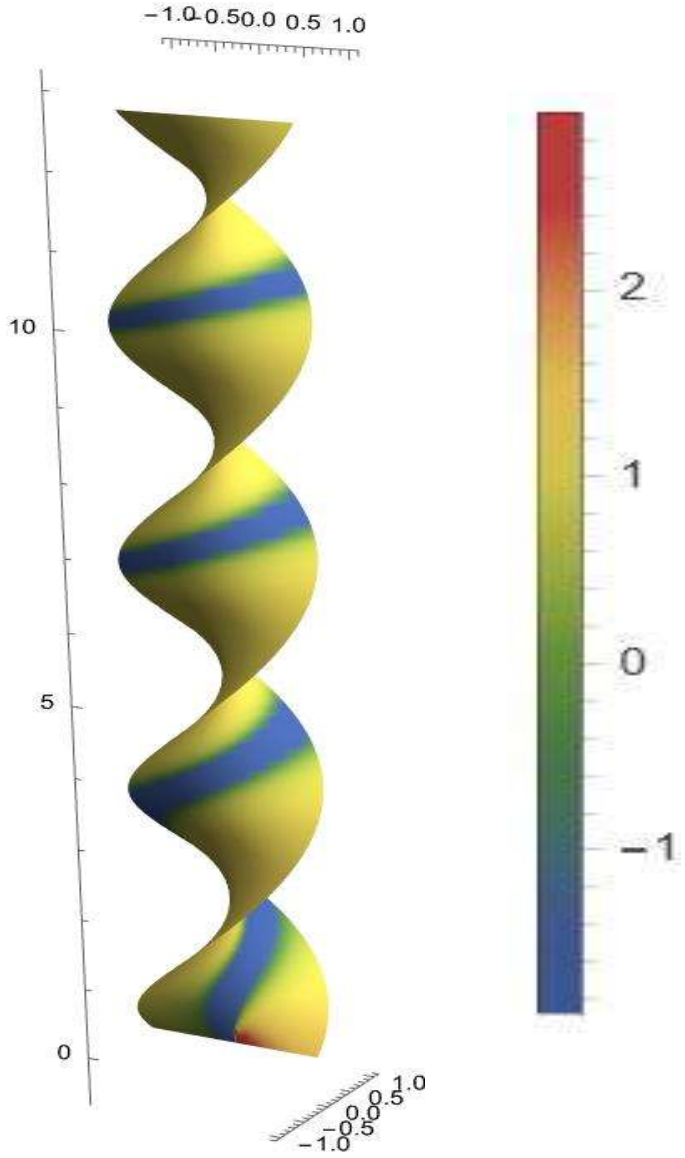

Figure 8: The mean DNA double helix curvature exists in yellow color and decreases in blue color.

6.2. A Cusp Surface

Consider $\rho: I \to \mathbb{R}^n$ a curve (potentially with ρ'_+ and ρ'_- as side derivatives). There are two distinct classifications of cusp in the literature [24]:

1. $\rho(t)$ is referred to as a cusp if $\rho'_+(t) = -\rho'_-(t) \neq 0$;
2. $\rho(t)$ is known as a cusp if $\rho'(t) = 0$ and $\rho''(t) \neq 0$.

Considering the two curves $\Psi_1(y) = (8,4,0)\, y^3 - (12,9,0)\, y^2 + (6,6,0)\, y + (-1,0,0)$ and $\Psi_2(y) = (2y-1,\ 4y(y-1),\ 1)$, describe a lofted surface that is simple to determine. Make a note of how the

curves transfer through the points $\Psi_1(0) = (-1,0,0), \Psi_1(0.5) = \left(0, \frac{5}{4}, 0\right), \Psi_1(1) = (1,1,0),\ \Psi_2(0) = (-1,0,1),\ \Psi_2(0{,}5) = (0,-1,1)$, and $\Psi_2(1) = (1,0,1)$, It facilitates the visualization of the surface (Figure 9). The two curves' tangent vectors [3] are:

$$\Psi_1^y(y) = (24,12,0)y^2 - (24,18,0)y + (6,6,0), \qquad \Psi_2^y(y) = (2,8y-4,0).$$

Observing that $\Psi_1^y(0.5) = (0,0,0)$, indicates that $\Psi_1(y)$ does have a cusp at $y = 0.5$ [3].

The lofted surface that the two curves describe is [3]:

$$\Psi(y,w) = (4\,y^2(2y-3)(1-w) - 4y\,w + 6y - 1,\ \ y^2(4y-9)(1-w) + 4y^2\,w - 10y\,w + 6y,\ \ w)$$

Figure 9: The lofted surface patch

We get some properties of a cusp lofted surface (first and second fundamental forms, mean curvature, Gaussian and second Gaussian curvatures, and Weingarten surface).

$$\wp_{11} = \big(6 - 24(-1+y)y(-1+w) - 4\,w + w\,\kappa_1(y)\big)^2 + \big(-2(-1+2y)(3+3y(-1+w) - 5w) + w\ \kappa_2(y)\big)^2,$$

$$\wp_{12} = -4(-1+y)\,y\,(-1+2y)\big(6 - 24(-1+y)y(-1+w) - 4w + w\,\kappa_1(y)\big) - (-2+y)y(-5+4y)\big(-2(-1+2y)(3+3y(-1+w) - 5w) + w\,\kappa_2(y)\big),$$

$$\wp_{22} = y^2\left(116 + y\left(-356 + y\left(457 + 8y\,(-37+10y)\right)\right)\right),$$

$$h_{11} = 4(-3 + 12(-1+y)y(-1+w) + 2w)\,\kappa_1(y) - w\,\kappa_1^2(y) + 4(-1+2y)(3+3y(-1+w) - 5w)\,\kappa_2(y) - w\kappa_2^2(y) + (-1+2y)(-1+4(-1+y)y(-1+w))\,\kappa_1'(y) + y(-6+y(9+4(-1+w) - 13w) + 10w)\,\kappa_2'(y),$$

$$h_{12} = 4(-1+y)y(-1+2y)\,\kappa_1(y) + (-2+y)y(-5+4y)\,\kappa_1(y), \qquad h_{22} = 0,$$

$$d = 2\Big(36 + 2y\big(-87 + 34w + 4y(33 - 15y - 16w + 7wy)\big) + (-2+y)(-5+4y)w\,\kappa_1(y) - 4(-1+y)(-1+2y)w\,\kappa_2(y)\Big)^2$$

$$H(y,w)=\frac{1}{d}\Big((-6+y+4y^2)\big(14+y(-25+12y)\big)w\,\kappa_1^2(y)$$
$$+16(-1+y)(-1+2y)\left(18+y\big(-87+34w+4y(33-15y-16v+7y\,w)\big)\right)\kappa_2(y)$$
$$-(-6+y+4y^2)(14+y(-25+12y))w\,\kappa_2^2(y)-4(-2+y)(-5+4y)\,\kappa_1(y)(18$$
$$+y\big(-87+34w+4y(33-15y-16w+7y\,w)\big)-4(-1+y)(-1+2y)w\,\kappa_2(y))$$
$$+\Big(116$$
$$+y\left(-356+y\big(457+8y(-37+10y)\big)\right)\Big)\Big((-1+2y)\big(-1$$
$$+4(-1+y)y(-1+w)\big)\,\kappa_1'(y)+y(-6+y(9+4y(-1+w)-13w)+10w)\,\kappa_2'(y)\Big)\Big)$$

$$M=y^2\left(36+2y\left(-87+34w+4y\big(33-16w+y(-15+7w)\big)\right)+(-2+y)(-5+4y)w\,\kappa_1(y)-4(-1+y)(-1+2y)w\,\kappa_2(y)\right)^2$$

$$K(y,w)=-\frac{\big(4(-1+y)y(-1+2y)\,\kappa_1(y)+(-2+y)y(-5+4y)\,\kappa_2(y)\big)^2}{M}$$

The cusp surface is a (H,K) Weingarten surface under the condition:

$$\frac{\kappa_1(y)}{\kappa_2(y)}=-\frac{(-2+u)(-5+4u)}{4(-1+u)(-1+2u)}.$$

The Gaussian and mean surface curvatures of the cusp are illustrated in Figures 10 and 11, respectively.

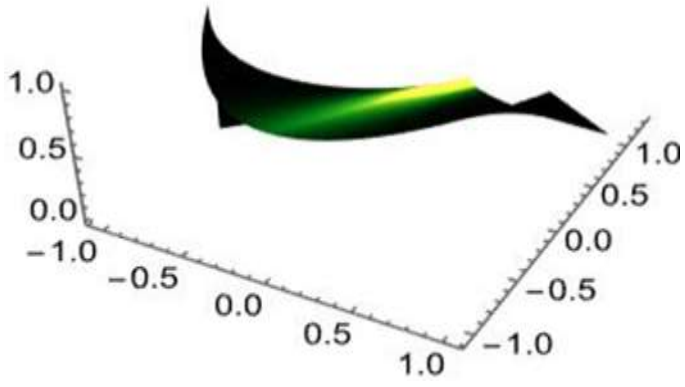

Figure 10: At the value of zero, the Gaussian curvature is not defined, and becomes green. it decreases gradually between the yellow and shamrock colors and appears in the values $2and$ above zero. The curvature decreases between pine color and juniper color appear between the values under zero value and -2.

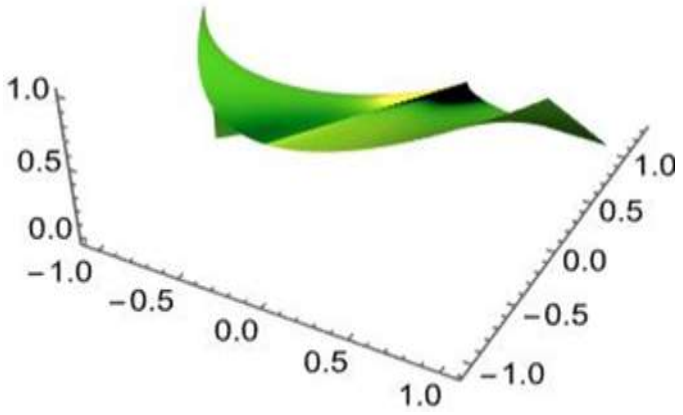

Figure 11: The gradient green color takes up most of the surface, and the mean curvature increases in the yellow color at values 2 and decreases very much at value -2 for the color juniper.

CONCLUSION

In this paper, we studied and designed the generation of the loft surface using three different curves. The loft surface properties were investigated using a type-2-Bishop frame in isotropic space. We discovered conditions to know when the surfaces are minimal, developable, and Weingarten surfaces by mean, Gaussian, and second Gaussian curvatures. We mentioned two applications in biology and geometry.

Acknowledgments

We are very grateful to the editor and the referees for their ideas and suggestions that helped us improve the paper.

Competing Of Interest

The authors declare that theyhave no competing of interest.

REFERENCES

[1] Prasad, KSRK, Selvaraj, P, Ayachit, PV, Nagamani, BV. On the development of lofts for doubly curved sheet metal components. Comput. Aided. Des. 2006; 6(1): 199-211. https://koreascience.or.kr/article/JAKO200634514932125.pdf

[2] Salomon, D. Linear Interpolation. In: Curves and surfaces for computer graphics. Springer Science & Business Media 2007; 49-69. https://link.springer.com/book/10.1007/0-387-28452-4

[3] Filkins, PC. Algorithms for blending surface generation. MASSACHUSETTS INST. OF TECH. CAMBRIDGE. 1991

https://upload.wikimedia.org/wikipedia/commons/e/ef/Algorithms_for_blending_surface_generation._%28IA_algorithmsforble00filk%29.pdf

[4] Chang, KH. Geometric Modeling in e-Design: computer-aided engineering design. Academic Press. 2016; 43-124. https://shop.elsevier.com/books/e-design/chang/978-0-12-809569-0

[5] Farin, G, Hoschek, J, Kim, MS, Eds. Handbook of computer-aided geometric design Elsevier 2002. ISBN 978-0-444-51104-1. https://shop.elsevier.com/books/handbook-of-computer-aided-geometric-design/farin/978-0-444-51104-1

[6] Schoonmaker SJ. The CAD guidebook: A basic manual for understanding and improving computer-aided design. CRC Press; 2002 Nov 5.

https://doi.org/10.1201/9780203911037.

[7] Farin, G. Curves and surfaces for CAGD: a practical guide. Morgan Kaufmann. 2002 ISBN 1-55860-737-4. https://www.cin.ufpe.br/~mdlm/files/Farin-5a_edicao.pdf

[8] Olasupo SB, Uzairu A, Shallangwa GA, Uba S. Computer-aided drug design and in silico pharmacokinetics predictions of some potential antipsychotic agents. Scientific African. 2021 Jul 1;12:e00734. https://www.researchgate.net/publication/349801673_Computer-aided_drug_design_and_in_silico_pharmacokinetics_predictions_of_some_potential_antipsychotic_agents

[9] As E, Sarıoğlugil A. On the Bishop curvatures of involute-evolute curve couple in. Int. J. Phys. Sci. 2014;9(7):140-5. https://doi.org/10.5897/IJPS2013.4079

[10] Bishop RL. There is more than one way to frame a curve. The American Mathematical Monthly. 1975 Mar 1;82(3):246-51. https://doi.org/10.1080/00029890.1975.11993807.

[11] Özyılmaz E. Classical differential geometry of curves according to type-2 Bishop trihedra. Mathematical and Computational Applications 2011 Dec;16(4):858-67. https://doi.org/10.3390/mca16040858.

[12] Farooq, A. J., Akhtar, S., Hijazi, S. T., & Khan, M. B. (2010). Impact of advertisement on children behavior: Evidence from pakistan. European Journal of Social Sciences, 12(4), 663-670.

[13] Körpinar, T, Asil, V, Sariaydin, MT, İncesu, M. A characterization for bishop equations of parallel curves according to Bishop Frame in E^3. Bol. Da Soc. Parana. De Mat 2015; 33(1), 33-39 https://doi.org/10.5269/bspm.v33i1.21712.

[14] Yılmaz, S, Turgut, M. A new version of Bishop frame and an application to spherical images. J. Math. Anal. Appl. 2010; 371(2), 764-776. https://doi.org/10.1016/j.jmaa.2010.06.012

[15] Soliman MA, Mahmoud WM, Solouma EM, Bary M. The new study of some characterization of canal surfaces with Weingarten and linear Weingarten types according to Bishop frame. Journal of the Egyptian Mathematical society. 2019 Dec;27(1):1-7. https://doi.org/10.1186/s42787-019-0032-y.

[16] Ro JS, Yoon DW. Tubes of Weingarten types in a Euclidean 3-space. Journal of the Chungcheong mathematical society. 2009 Aug 15;22(3):359. https://doi.org/10.14403/jcms.2014.27.3.403

[17] Milin Šipuš Ž. Translation surfaces of constant curvatures in a simply isotropic space. Periodica Mathematica Hungarica. 2014 Jun;68(2):160-75. https://doi.org/10.1007/s10998-014-0027-2.

[18] Aydin ME. A generalization of translation surfaces with constant curvature in the isotropic space. Journal of Geometry. 2016 Dec;107(3):603-15. https://link.springer.com/article/10.1007/s00022-015-0292-0

[19] Karacan MK, Yoon DW, Bukcu B. Translation surfaces in the three-dimensional simply isotropic space I_3^1. International Journal of Geometric Methods in Modern Physics. 2016 Aug 12;13(07):1650088. https://doi.org/10.1142/S0219887816500882.

[20] Solouma EM, Wageeda MM, Soliman MA, Bary M. Geometric Properties of Special Spacelike Curves in Three-Dimension Minkowski Space-Time. Modern Applied Science.2020;14(2):1-11. https://ccsenet.org/journal/index.php/mas/article/view/0/41836

[21] Ibrahim AL, Solouma E, Khan M. On geometry of focal surfaces due to B-Darboux and type-2 Bishop frames in Euclidean 3-space. AIMS Mathematics. 2022;7(7):13454-13468. http://doi.org/10.3934/math.2022744.

[22] Watson JD, Crick FH. Molecular structure of nucleic acids: a structure for deoxyribose nucleic acid. Nature. 1953 Apr 25;171(4356):737-738. https://pubmed.ncbi.nlm.nih.gov/13054692/

[23] Drew HR, Wing RM, Takano T, Broka C, Tanaka S, Itakura K, Dickerson RE. Structure of a B-DNA dodecamer: conformation and dynamics. Proceedings of the National Academy of Sciences. 1981 Apr;78(4):2179-2183. https://pubmed.ncbi.nlm.nih.gov/6941276/

[24] Pray L. Discovery of DNA structure and function: Watson and Crick. Nature Education 2008;1(1):100. https://www.nature.com/scitable/topicpage/discovery-of-dna-structure-and-function-watson-397/.

[25] Almeida R, Neves V, Stroyan K. Infinitesimal differential geometry: cusps and envelopes. Differ. Geom. Dyn. Syst. 2014 Jan 1;16:1-3. http://www.mathem.pub.ro/dgds/v16/D16-al-279.pdf

DOI: https://doi.org/10.15379/ijmst.v10i3.1864